

## **Accelerated Epigenetic Aging is Associated with Faster Glaucoma Progression: A DNA Methylation Study**

Felipe A. Medeiros, MD, PhD<sup>1,2</sup>, Achintya Varma, MS<sup>3</sup>, Alessandro A. Jammal, MD, PhD<sup>1</sup>,  
Henry Tseng, MD, PhD<sup>2</sup>, William K. Scott, PhD<sup>3,4</sup>

1. Bascom Palmer Eye Institute, University of Miami, Miami, FL
2. Duke Eye Center and Department of Ophthalmology, Duke University, Durham, NC
3. John P. Hussman Institute for Human Genomics, University of Miami, FL
4. Dr. John T. MacDonald Foundation Department of Human Genetics, University of Miami, FL

**Financial Support:** Supported in part by National Institutes of Health/National Eye Institute grant EY029885 (F.A.M), Aging Team Science Grant from the University of Miami (F.A.M), Shaffer Grant from the Glaucoma Research Foundation (F.A.M). The funding organizations had no role in the design or conduct of this research.

**Financial Disclosures:** F.A.M.: AbbVie (C), Annexon (C); Carl Zeiss Meditec (C), Galimedix (C); Google Inc. (F); Heidelberg Engineering (F), nGoggle Inc. (P), Novartis (F); Stealth Biotherapeutics (C); Stuart Therapeutics (C), Thea Pharmaceuticals (C), Reichert (C, F). A.V.: None. A.A.J.: None. H.T.: Novartis (F). W.K.S.: None.

**Abbreviations:** Age acceleration (AgeAccel); central corneal thickness (CCT); cytosine-phosphate-guanine (CpG); Duke Glaucoma Registry (DGR); Goldmann applanation tonometry (GAT); intraocular pressure (IOP); international classification of diseases (ICD); mean deviation (MD); primary open-angle glaucoma (POAG); retinal nerve fiber layer (RNFL) standard automated perimetry (SAP); Swedish Interactive Thresholding Algorithm (SITA).

**Correspondence:** Felipe A. Medeiros, MD, PhD, Bascom Palmer Eye Institute, 900 NW 17<sup>th</sup> St, Miami, FL. E-mail: [fmedeiros@med.miami.edu](mailto:fmedeiros@med.miami.edu)

1 **ABSTRACT**

2

3 **Purpose:** To investigate the association between epigenetic age acceleration and glaucoma  
4 progression.

5 **Design:** Retrospective cohort study.

6 **Participants:** 100 primary open-angle glaucoma (POAG) patients with fast progression and 100  
7 POAG patients with slow progression.

8 **Methods:** Subjects were classified as fast or slow progressors based on rates of change in  
9 standard automated perimetry (SAP) mean deviation (MD) and retinal nerve fiber layer (RNFL)  
10 thickness. Epigenetic age was calculated using the Horvath, Hannum, PhenoAge, and GrimAge  
11 clocks from DNA methylation profiles obtained from blood samples. Age acceleration  
12 (AgeAccel) was defined as the residual from a linear regression of epigenetic age on chronologic  
13 age, with positive values suggesting faster biological aging. Multivariable logistic regression  
14 models estimated the association between AgeAccel and likelihood of fast progression, adjusting  
15 for confounders.

16 **Main Outcome Measures:** Difference in epigenetic age acceleration between fast and slow  
17 glaucoma progressors.

18 **Results:** The mean rate of SAP MD change in the fastest progressing eye was -1.06 dB/year  
19 (95% CI: -1.28 to -0.85) for fast progressors compared to -0.10 dB/year (95% CI: -0.16 to -0.04)  
20 for slow progressors (P<0.001). For RNFL thickness, corresponding values were -1.60 µm/year  
21 (95% CI: -1.97 to -1.23) and -0.76 µm/year (95% CI: -1.04 to -0.48), respectively (P<0.001).

22 Fast progressors demonstrated significantly greater age acceleration compared to slow  
23 progressors for the Horvath clock (mean difference = 2.93 years, 95% CI: 1.48 to 4.39, P<0.001)  
24 and Hannum clock (mean difference = 1.24 years, 95% CI: 0.03 to 2.46, P=0.045). In  
25 multivariable models, each year of Horvath AgeAccel was associated with 15% higher odds of  
26 fast progression (OR 1.15, 95% CI 1.07-1.23, P<0.001), after adjusting for sex, race, intraocular  
27 pressure, central corneal thickness, baseline disease severity, smoking status and follow-up time.  
28 Hannum and GrimAge clocks also showed significant associations with fast progression. The  
29 association between AgeAccel and fast progression was stronger in subjects with relatively low  
30 IOP during follow-up.

31 **Conclusion:** Accelerated epigenetic aging was associated with faster glaucoma progression.  
32 These findings suggest that faster biological age, as reflected in DNA methylation, may increase  
33 optic nerve susceptibility to damage, highlighting epigenetic age as a potential prognostic  
34 biomarker.

35

## 36 INTRODUCTION

37

38           Glaucoma is a neurodegenerative disease characterized by progressive loss of retinal  
39 ganglion cells and their axons.<sup>1</sup> The disease affects over 100 million individuals worldwide and  
40 is the leading cause of irreversible blindness. Although elevated intraocular pressure (IOP) is the  
41 most widely accepted modifiable risk factor for glaucoma, a significant proportion of patients  
42 continue to experience glaucomatous deterioration despite well-controlled IOP, suggesting that  
43 other factors contribute to the progression of glaucomatous damage.<sup>2</sup> Moreover, a subset of 30%  
44 to 40% of patients exhibits normal-tension glaucoma, where damage occurs without concomitant  
45 apparent IOP elevation. This indicates that factors other than IOP elevation may increase the  
46 optic nerve's susceptibility to damage.<sup>3</sup>

47           Aging plays a pivotal role in glaucoma. The prevalence of glaucoma increases markedly  
48 with age.<sup>4,5</sup> However, the pathophysiology underlying increasing age as a risk factor for  
49 glaucoma is not well understood. The increased prevalence of glaucoma in older individuals does  
50 not seem to be explained solely by an increased prevalence of high IOP with aging.<sup>6-8</sup> This  
51 suggests that aging may increase the vulnerability of the optic nerve to IOP-related damage,  
52 ultimately resulting in loss of retinal ganglion cells. This age-related increased vulnerability to  
53 neural injury has also been observed in other neurodegenerative disorders, such as Alzheimer's  
54 and Parkinson's disease, and may be related to mitochondrial dysfunction and impaired capacity  
55 to handle oxidative stress, among other factors.<sup>9-15</sup> Epigenetics, the study of alterations in gene  
56 expression without changes in the DNA sequence, has shown promise in understanding aging  
57 and age-related diseases. The biological age encapsulated in our epigenome, as reflected by DNA  
58 methylation patterns, often diverges from our chronological age. The "epigenetic clock" theory,

59 conceptualized by Horvath,<sup>16</sup> leverages these methylation changes at specific cytosine-  
60 phosphate-guanine (CpG) sites as a timekeeper of biological aging. The disparities between  
61 biological (epigenetic) and chronological age have been associated with several age-related  
62 diseases, such as cardiovascular disease, neurodegeneration, and cancer. An advanced epigenetic  
63 age relative to chronological age may signify accelerated biological aging and increased disease  
64 risk.<sup>17</sup> Despite these observations, no study has yet been conducted on epigenetic age and  
65 glaucoma.

66 In the present study, we hypothesized that disparities between epigenetic and  
67 chronological age may be a significant risk factor in explaining glaucoma progression.  
68 Specifically, we hypothesized that individuals with faster disease progression would demonstrate  
69 an accelerated biological age, as indicated by a greater divergence between epigenetic and  
70 chronological age, compared to those with slower progression. Uncovering the relationship  
71 between epigenetic age and glaucoma progression could provide novel insights into the  
72 pathophysiology of the disease and offer a more accurate prognostic tool than chronological age  
73 alone.

74

## 75 **METHODS**

76 This study involved a cohort of subjects that were part of the Duke Glaucoma Registry  
77 (DGR), a large database of electronic medical records developed at Duke University, Durham,  
78 North Carolina. The database consisted of adults 18 years or older with glaucoma or glaucoma  
79 suspect diagnoses who were evaluated at the Duke Eye Center or its satellite clinics between  
80 January 2009 and June 2023. The database has been described in detail elsewhere and has been

81 used for several studies investigating risk factors for glaucoma.<sup>3, 18-21</sup> A subset of participants,  
82 described below, was recruited for blood sample collection. Blood sample analyses were  
83 performed at the John P. Hussman Institute for Human Genomics (HIHG) at the University of  
84 Miami, Florida. The Duke University and the University of Miami Institutional Review Boards  
85 approved this study. Informed consent was obtained from all participants. All methods adhered to  
86 the tenets of the Declaration of Helsinki for research involving human subjects and were  
87 conducted in accordance with regulations of the Health Insurance Portability and Accountability  
88 Act.

89         The database used for this study contained clinical information from baseline and follow-  
90 up visits, including patient diagnostic and procedure codes, medical history, smoking history,  
91 best-corrected visual acuity, slit-lamp biomicroscopy, IOP measurement using the Goldmann  
92 applanation tonometry (GAT; Haag-Streit, Konig, Switzerland), central corneal thickness (CCT),  
93 gonioscopy, ophthalmoscopy examination, optic disc photographs, and the results of all standard  
94 automated perimetry (SAP) and optical coherence tomography (OCT) exams. SAP testing was  
95 performed with the Humphrey Field Analyzer (Carl Zeiss Meditec, Dublin, CA) using the  
96 Swedish Interactive Thresholding Algorithm (SITA) 24-2 fast strategy. OCT was performed with  
97 the Spectralis SDOCT (Heidelberg Engineering, Dossenheim, Germany). A reliable SAP was  
98 defined as having fixation loss rate less than 25% and false-positive rate less than 15%. Visual  
99 fields were manually reviewed for artifacts such as lid and rim artifacts, fatigue effects,  
100 inappropriate fixation, and evidence that the visual field results were due to a disease other than  
101 glaucoma. Retinal nerve fiber layer (RNFL) thickness measurements were obtained from a 12-  
102 degree (for single circle scans) or a 3.45mm-diameter peripapillary circle scan (for scans from  
103 the Glaucoma Mode Premium Edition) acquired using the Spectralis SD OCT, as described in

104 detail previously.<sup>22</sup> Tests were acquired using the latest available software version at the time of  
105 the scan and exported using the latest available version at the time of the analysis (Software  
106 version 6.8). Scans were manually reviewed for the presence of artifacts, decentration, or  
107 segmentation errors. Tests with quality score below 15, or with segmentation errors, evidence of  
108 decentration or artifacts were also excluded. For each scan, the global average RNFL thickness  
109 was calculated as the average of thicknesses of all points from the 360 degrees around the optic  
110 nerve head.

### 111 *Participant selection*

112 This study included a subset of participants from the DGR who were recruited for  
113 prospective blood sample collection. Subjects were contacted during their regular clinic visits  
114 and invited to provide blood samples for genetic analysis. Selection criteria included a diagnosis  
115 of primary open-angle glaucoma (POAG) in both eyes, confirmed by international classification  
116 of diseases (ICD) codes at the baseline visit, as well as the availability of longitudinal data in the  
117 DGR. 1,251 POAG patients provided blood samples. A total of 10 ml of blood was collected  
118 from each participant, processed, and stored for future analysis. Blood collections took place  
119 between June 2021 and June 2023.

### 120 *Fast versus slow progression classification*

121 Subjects were classified as either fast or slow progressors based on available SAP and SD  
122 OCT tests. Ordinary least squares linear regression was used to estimate the slopes of change in  
123 SAP mean deviation (MD) and RNFL thickness over time. Subjects who did not clearly fit into  
124 either group were excluded from further analyses to maximize the distinction between fast and  
125 slow progressors and avoid including ambiguous cases. Fast progressors were defined as having

126 at least one eye with either a statistically significant SAP MD slope faster than -0.5 dB/year or a  
127 statistically significant global RNFL thickness slope faster than -1.0  $\mu\text{m}/\text{year}$ . In contrast, slow  
128 progressors were required to meet all of the following criteria in both eyes: non-significant SAP  
129 MD slope, non-significant global RNFL thickness slope, a minimum follow-up time of 5 years,  
130 and no history of trabeculectomy or tube shunt surgery.

131 These criteria were designed to create a clearly divergent sample, thereby enhancing the  
132 ability to test the primary hypothesis of the study. No minimum follow-up time was required for  
133 fast progressors, allowing the inclusion of patients with rapid progression over shorter periods.  
134 While a history of glaucoma surgery was not an exclusion criterion for fast progressors, SAP and  
135 OCT tests were censored post-surgery and excluded from the calculation of progression rates.  
136 Importantly, we use the term 'slow progressor' rather than 'non-progressor' because it is not  
137 possible to guarantee that these subjects would not have progressed by other measures. The  
138 primary objective was to ensure that any changes in the slow progressor group would likely be  
139 minimal, resulting in a significant difference in disease trajectory between the two groups.

#### 140 *Sample Size Calculation*

141 The primary hypothesis of this study was that individuals with faster glaucoma  
142 progression would demonstrate an accelerated biological age, indicated by a greater discrepancy  
143 between epigenetic age and chronological age, compared to those with slower progression.  
144 Given the high costs associated with DNA methylation analysis, only a subset of subjects with  
145 available blood samples underwent epigenetic age calculation. A power analysis determined that  
146 a sample size of 100 subjects per group would provide 80% power to detect a minimum  
147 difference of 2.0 years between the two groups in the difference between epigenetic and  
148 chronological age, assuming a standard deviation of 5.0 and an alpha level of 0.05.

149 Consequently, from the 1,251 subjects with available blood samples, 100 individuals with slow  
150 progression and 100 with fast progression were selected. These 200 samples were then subjected  
151 to DNA extraction, methylation profiling and epigenetic age calculation.

### 152 *DNA Extraction, Methylation Processing, and Quality Control*

153 Immediately after collection, whole blood samples were centrifuged to separate the  
154 different components. The separated components, including plasma, buffy coat, and red blood  
155 cells, were then frozen at -80°C for preservation. At a later stage, the buffy coat was thawed and  
156 processed for DNA extraction. Upon thawing, the buffy coat was centrifuged at 1,500 x g for 10  
157 minutes to concentrate the cells. Genomic DNA was subsequently extracted from the buffy coat  
158 using the QIAamp DNA Blood Mini Kit (Qiagen, Hilden, Germany), following the  
159 manufacturer's protocol. The quality of the extracted DNA was assessed using a NanoDrop  
160 spectrophotometer (Thermo Fisher Scientific, Waltham, MA). The absorbance ratios at 260/280  
161 nm and 260/230 nm were measured, with DNA samples considered high quality if the A<sub>260/280</sub>  
162 ratio fell between 1.8 and 2.0, and the A<sub>260/230</sub> ratio was  $\geq 2.0$ . The quantity and concentration  
163 of DNA were evaluated using a Qubit Fluorometer (Thermo Fisher Scientific, Waltham, MA).  
164 Additionally, DNA integrity was qualitatively evaluated using agarose gel electrophoresis to  
165 identify samples with high molecular weight bands suitable for analysis. Sample concentration  
166 was normalized to 50 ng/ $\mu$ L and arrayed in Azenta 0.5 ml barcoded tubes in racks of 96.

167 Genome-wide DNA methylation was assessed using the Illumina Infinium  
168 MethylationEPIC v2 BeadChip (Illumina, San Diego, CA), which interrogates approximately  
169 930,000 cytosine-phosphate-guanine (CpG) sites across the human genome. DNA samples (500  
170 ng each) were bisulfite-converted using the EZ DNA Methylation Kit (Zymo Research, Irvine,  
171 CA) according to the manufacturer's instructions, which converts unmethylated cytosines to



172 uracil while leaving methylated cytosines unchanged. The bisulfite-converted DNA was then  
173 hybridized to the MethylationEPIC v2 BeadChip, and the arrays were scanned using the Illumina  
174 iScan system. Data files created by the Illumina iScan were analyzed using the Illumina  
175 GenomeStudio Methylation module software program. To ensure the reliability of the  
176 methylation data, several quality control measures were implemented following established  
177 protocols in the literature. Raw methylation intensity data were first preprocessed using the R  
178 package minfi, which includes background correction, normalization, and calculation of  
179 detection p-values to assess the quality of individual probes.<sup>23</sup> Probes with detection p-values  
180 above a threshold of 0.01 in more than 5% of samples were excluded from further analysis.<sup>24</sup>  
181 Methylation data were then mapped to the genome, and only those probes that passed stringent  
182 quality control criteria were retained for epigenetic age calculation.

### 183 *Epigenetic Age Calculation*

184 Epigenetic age was calculated using several established algorithms, each of which applies  
185 specific sets of CpG sites to estimate biological age:

- 186 • **Horvath Clock:** The Horvath clock is an epigenetic age estimator that utilizes a linear  
187 combination of methylation levels at 353 specific CpG sites to calculate an individual's  
188 biological age; these sites were selected from data generated from multiple tissue types,  
189 including blood, skin, brain and other internal organs.<sup>25</sup> This "universal" epigenetic clock  
190 is designed to provide a robust estimate of biological age, regardless of tissue source, and  
191 has been widely validated for its accuracy in correlating with chronological age across a  
192 diverse range of tissues.
- 193 • **Hannum Clock:** The Hannum clock is an epigenetic age predictor specifically tailored  
194 for use in whole blood samples.<sup>26</sup> It is based on methylation data from 71 CpG sites that

195 are strongly associated with age-related changes in blood. The model calculates  
196 biological age by assessing methylation patterns at these sites, which reflect the  
197 physiological aging process in hematopoietic cells, making it potentially useful for  
198 studies focusing on blood-based biomarkers of aging.

- 199 • **PhenoAge:** The PhenoAge clock, developed by Levine et al.,<sup>27</sup> integrates DNA  
200 methylation data from 513 CpG sites with clinical phenotypes and mortality risk  
201 indicators to provide a comprehensive measure of biological aging. Unlike traditional  
202 epigenetic clocks that primarily estimate chronological age, PhenoAge is designed to  
203 capture the physiological decline associated with morbidity and mortality risk.
- 204 • **GrimAge:** GrimAge is an epigenetic clock that combines methylation data from specific  
205 CpG sites with inferred plasma protein levels and cumulative smoking exposure to  
206 predict time to death and other aging-related outcomes.<sup>28</sup>

207 Methylation data for the probes was submitted to the DNA Methylation Age Calculator  
208 website ([dnamage.clockfoundation.org](http://dnamage.clockfoundation.org)).<sup>25</sup> For each one of these clocks, age acceleration  
209 (AgeAccel) was calculated as the residual from a linear regression model of the corresponding  
210 epigenetic clock and chronological age. Residual variables were then named AgeAccelHorvath,  
211 AgeAccelHannum, AgeAccelPheno and AgeAccelGrim, corresponding to the clocks listed  
212 above. Positive values in these variables suggest a higher epigenetic age relative to chronological  
213 age and thus faster biological aging, while negative values suggest slower biological aging.

## 214 *Statistical Analysis*

215 Correlations between chronological age and each epigenetic age measure were assessed  
216 using Pearson's correlation coefficients. Differences in AgeAccel (epigenetic age acceleration)  
217 between fast and slow glaucoma progressors were evaluated using Student's t-tests. Additionally,

218 multivariable logistic regression models were employed to estimate adjusted odds ratios (ORs)  
219 and 95% confidence intervals (CIs) for the association between AgeAccel variables and the  
220 likelihood of fast progression. These models were adjusted for key potential confounders,  
221 including gender, race, smoking status, IOP, CCT, and baseline disease severity, as measured by  
222 baseline MD. For IOP, both the mean and peak values recorded during follow-up were analyzed.  
223 Since IOP, CCT, and baseline MD are eye-specific variables, the mean values of both eyes were  
224 utilized in the logistic regression models. Furthermore, considering that blood samples were  
225 collected during follow-up rather than at baseline, the time from baseline to the date of blood  
226 collection was calculated and included as a potential confounder in the multivariable models.

227         Statistical analyses were completed in R (version 4.4.1, R Foundation for Statistical  
228 Computing, Vienna, Austria).

229

## 230 **RESULTS**

231         The study included 100 POAG patients diagnosed with fast glaucoma progression and  
232 100 POAG patients with slow progression. **Table 1** shows demographic and clinical  
233 characteristics of the 2 groups. Mean follow-up time was 10.3 years (95% CI: 9.0 – 11.5) for fast  
234 progressors and 11.0 years (95% CI: 9.6 – 12.3) for slow progressors, with no statistically  
235 significant difference between the groups ( $P = 0.45$ ). The mean rate of change in SAP MD,  
236 averaged across both eyes, was significantly different between the groups: -0.63 dB/year (95%  
237 CI: -0.77 – -0.48) in fast progressors compared to 0.01 dB/year (95% CI: -0.06 – 0.07) in slow  
238 progressors ( $P < 0.001$ ). When considering the eye with the faster rate of SAP MD decline, the  
239 mean rates were -1.06 dB/year (95% CI: -1.28 – -0.85) for fast progressors and -0.10 dB/year

240 (95% CI: -0.16 – -0.04) for slow progressors ( $P < 0.001$ ). Over the follow-up period, fast  
241 progressors lost an average of 8.2 dB (95% CI: 6.9 – 9.5) of MD in the fastest progressing eye,  
242 compared to a loss of only 1.4 dB (95% CI: 0.8 – 1.9) in the slow progressor group. For OCT  
243 RNFL thickness, the mean rate of change in the fastest progressing eye was  $-1.60 \mu\text{m}/\text{year}$  (95%  
244 CI:  $-1.97 - -1.23$ ) for fast progressors, compared to  $-0.76$  (95% CI:  $-1.04 - -0.48$ )  $\mu\text{m}/\text{year}$  for  
245 slow progressors ( $P < 0.001$ ). Mean IOP during follow-up was similar between the groups, at  
246 15.0 mmHg (95% CI: 14.4 – 15.6) for fast progressors and 15.3 mmHg (95% CI: 14.7 – 16.0) for  
247 slow progressors ( $P = 0.39$ ). However, peak IOP during follow-up, averaged across both eyes,  
248 was higher in fast progressors compared to slow progressors (23.8 mmHg [95% CI: 22.0 – 25.5]  
249 vs. 20.5 mmHg [95% CI: 19.5 – 21.6], respectively;  $P = 0.002$ ).

250 Epigenetic age was strongly correlated with chronological age across all epigenetic clock  
251 methods (**Figure 1**). The Horvath clock showed a Pearson correlation coefficient of  $r = 0.83$   
252 (95% CI: 0.78 – 0.87) with chronological age ( $P < 0.001$ ). Similarly, the Hannum clock  
253 demonstrated a correlation of  $r = 0.85$  (95% CI: 0.80 – 0.90;  $P < 0.001$ ), while the PhenoAge  
254 clock showed a correlation of  $r = 0.81$  (95% CI: 0.76 – 0.87;  $P < 0.001$ ). The GrimAge clock had  
255 a slightly lower but still substantial correlation with chronological age ( $r = 0.70$ ; 95% CI: 0.62 –  
256 0.78;  $P < 0.001$ ).

257 **Table 2** shows the mean age acceleration values for fast and slow progressors according  
258 to the different epigenetic clocks, while **Figure 2** shows the distribution of these values across  
259 the two groups. For AgeAccelHorvath, fast progressors had significantly greater age acceleration  
260 compared to those with slow progression, with a mean difference of 2.93 years (95% CI: 1.48 to  
261 4.39;  $P < 0.001$ ). Similarly, faster acceleration was observed with AgeAccelHannum, with a  
262 mean difference of 1.24 years (95% CI: 0.03 to 2.46;  $P = 0.045$ ). No statistically significant

263 differences were found for AgeAccelPheno or AgeAccelGrim. For AgeAccelPheno, the mean  
264 difference between fast and slow progressors was 1.06 years (95% CI: -0.51 to 2.64; P = 0.185).  
265 Likewise, AgeAccelGrim showed a mean difference of 1.49 years (95% CI: -0.17 to 3.14; P =  
266 0.079), which also did not reach statistical significance.

267 **Table 3** shows the results of multivariable logistic regression models for the association  
268 between different age acceleration variables and the likelihood of fast progression, adjusted for  
269 relevant covariates. AgeAccelHorvath demonstrated the strongest association with fast  
270 progression (OR: 1.15 per year of acceleration, 95% CI: 1.07-1.23, P<0.001). AgeAccelHanum  
271 and AgeAccelGrim also showed significant associations (OR: 1.07, 95% CI: 1.00-1.15, P=0.049  
272 and OR: 1.07, 95% CI: 1.01-1.14, P=0.034, respectively). AgeAccelPheno did not reach  
273 statistical significance (OR: 1.04, 95% CI: 0.99-1.10, P=0.141). Lower baseline MD, indicating  
274 worse severity at baseline, was significantly associated with fast progression across all models  
275 (OR ranging from 1.12 to 1.13 per dB lower, P=0.001 for all models). Peak IOP was also a  
276 significant predictor in all models, with the OR consistently at 1.09 or 1.10 per mmHg increase  
277 (P≤0.001 for all models). Male sex showed a trend towards higher odds of fast progression,  
278 although this did not reach statistical significance. CCT, race, follow-up time, and smoking status  
279 were not significantly associated with fast progression in any of the models.

280 We further examined the effect of age acceleration on the likelihood of fast progression in  
281 POAG subjects who had no history of elevated IOP, defined as those with both eyes never  
282 exceeding an IOP of 21 mmHg (**Table 4, supplemental**). Statistically significant differences  
283 were observed across all age acceleration metrics, except for AgeAccelPheno. Specifically, for  
284 AgeAccelHorvath, the mean difference between fast and slow progressors was 4.69 years (95%  
285 CI: 2.46 to 6.93), indicating acceleration in epigenetic aging among fast progressors.

286

## 287 **DISCUSSION**

288           To our knowledge, this study is the first to explore the link between epigenetic age and  
289 glaucoma progression, offering new insights into the role of biological aging in this  
290 neurodegenerative disease. Our findings revealed a significant association between accelerated  
291 epigenetic age and faster glaucoma progression, suggesting that biological aging processes may  
292 increase optic nerve susceptibility to glaucomatous damage.

293           The characterization of fast and slow progressors in our study was rigorous and designed  
294 to create a clearly divergent sample, enhancing the ability to test our primary hypothesis. The  
295 marked contrast in rates of change between fast and slow progressors ( $-1.06 \pm 1.08$  dB/year vs -  
296  $0.10 \pm 0.33$  dB/year in the fastest progressing eye, respectively) highlights the clinical  
297 significance of our findings and validates our sample construction strategy. Over the follow-up  
298 period, fast progressors lost an average of 8.2 dB in MD in their fastest progressing eye,  
299 compared to only 1.4 dB in the slow progressor group, highlighting the substantial difference in  
300 disease trajectory between these groups.

301           As expected, all epigenetic clocks demonstrated strong correlations with chronological  
302 age in our study population, with Pearson correlation coefficients ranging from 0.70 to 0.85.  
303 Following previously established methods, we calculated age acceleration as the residual from a  
304 linear regression model of each epigenetic clock and chronological age.<sup>25</sup> This allowed us to  
305 quantify the degree to which an individual's biological age, as measured by DNA methylation  
306 patterns, deviates from their chronological age. Using these age acceleration measures, our  
307 results demonstrated that individuals with faster glaucoma progression exhibited accelerated

308 biological aging, as indicated by the various epigenetic clocks. The Horvath clock showed the  
309 strongest association, with fast progressors demonstrating a mean age acceleration of almost 3  
310 years compared to slow progressors. This finding was further supported by the multivariable  
311 logistic regression model, which showed that for each year of age acceleration according to the  
312 Horvath clock, the odds of fast progression increased by 15% (OR: 1.15, 95% CI: 1.07-1.23,  
313  $P < 0.001$ ), after controlling for other clinical and demographic variables that potentially affect  
314 progression speed.

315         The stronger association observed with the Horvath clock may be attributed to its  
316 "universal" nature. Horvath developed this epigenetic clock using samples from 51 different  
317 tissues and cell types, including brain, whole blood, heart, kidney, liver, lung, among others.<sup>25</sup>  
318 While it did not specifically include eye tissue, it did incorporate brain tissue samples, which  
319 may be particularly relevant given the neurodegenerative nature of glaucoma. The Horvath  
320 clock's ability to predict age across diverse tissues suggests it captures fundamental aging  
321 processes that may be applicable to the eye and optic nerve. This universality might explain its  
322 stronger association with glaucoma progression in our study, as it likely reflects systemic aging  
323 processes that could affect the vulnerability of retinal ganglion cells and their axons. The  
324 Hannum clock, specifically designed for blood samples, also showed a significant association,  
325 albeit weaker than the Horvath clock. Interestingly, the PhenoAge clock showed the weakest  
326 association, likely due to its construction. PhenoAge incorporates clinical phenotypes and  
327 mortality risk indicators, such as albumin, creatinine, glucose, and inflammatory markers, which  
328 may not be directly linked to glaucomatous damage.<sup>27</sup> While these markers are relevant to  
329 overall health and aging, their connection to the specific mechanisms of glaucoma may be  
330 limited. The GrimAge clock, which showed an intermediate association, was developed to

331 predict mortality and health span using DNA methylation-based biomarkers for plasma proteins  
332 and smoking history.<sup>28</sup> Some of these factors, like smoking, may be relevant to glaucoma  
333 progression, while others may not directly influence optic nerve vulnerability, potentially  
334 explaining its intermediate performance.

335         The association between accelerated biological age and faster glaucoma progression may  
336 be explained by several mechanisms. Advanced biological age could increase the susceptibility  
337 of the optic nerve to damage due to a reduced ability to handle oxidative stress, which is  
338 recognized as a contributing factor to glaucomatous neurodegeneration.<sup>1</sup> Aging is associated with  
339 mitochondrial dysfunction and decreased antioxidant defenses, potentially making retinal  
340 ganglion cells more vulnerable to IOP-related stress.<sup>29-33</sup> Additionally, age-related biomechanical  
341 changes in the lamina cribrosa and peripapillary sclera could alter the optic nerve head response  
342 to IOP, potentially increasing susceptibility to axonal damage.<sup>14, 34</sup>

343         Our study found that age acceleration remained a significant predictor of fast glaucoma  
344 progression, even after adjusting for known risk factors such as IOP and baseline disease  
345 severity. The association of IOP and baseline MD with fast progression found in our models is  
346 similar to previous studies, supporting our approach. However, the independent association of  
347 epigenetic age acceleration suggests that biological aging contributes additional risk beyond  
348 these established factors. The observed differences in epigenetic age acceleration between fast  
349 and slow progressors were clinically significant, as depicted in the probability plot (**Figure 3**).  
350 This plot, based on the Horvath clock and adjusted for key confounders such as sex, race, peak  
351 IOP, baseline disease severity, CCT, and follow-up time, demonstrated a strong association  
352 between age acceleration and the likelihood of fast glaucoma progression. A 10-year increase in  
353 age acceleration was associated with a substantial increase in the probability of fast progression,



354 nearly doubling it. For example, at an age acceleration of approximately +10 years, the  
355 probability of fast progression approached 70%. These findings highlight the potential clinical  
356 importance of epigenetic age acceleration as a predictor of glaucoma progression, beyond the  
357 influence of established risk factors.

358         A particularly interesting finding was the stronger association between age acceleration  
359 and fast progression in subjects with low IOP, i.e., those who never had IOP greater than  
360 21mmHg. This aligns with clinical observations that low-pressure glaucoma is rarely seen in  
361 young individuals and supports the notion that biological aging may increase the optic nerve  
362 susceptibility to damage even at normal IOP levels. The mean difference in AgeAccelHorvath  
363 between fast and slow progressors in this subgroup was almost 5 years, substantially larger than  
364 in the overall cohort, emphasizing the potential importance of biological aging in these cases.

365         The association between accelerated biological aging and increased susceptibility to  
366 damage is not unique to glaucoma and has been observed in other neurodegenerative diseases.  
367 For instance, in Alzheimer's disease (AD), previous studies have found associations between  
368 epigenetic age acceleration and disease risk or progression.<sup>35,36</sup> Levine et al. reported that  
369 individuals with greater epigenetic age acceleration in brain tissue showed more rapid  
370 progression of AD neuropathology.<sup>35</sup> Similarly, McCartney et al. found that DNA methylation  
371 age acceleration in blood was associated with cognitive decline and dementia risk.<sup>36</sup> In  
372 Parkinson's disease, another neurodegenerative condition, Horvath and Ritz reported that patients  
373 exhibited accelerated epigenetic aging in brain tissues compared to controls.<sup>37</sup> These parallels  
374 with other neurodegenerative diseases support the notion that accelerated biological aging may  
375 increase susceptibility to neuronal damage across various conditions, including glaucoma.

376           The association between accelerated biological aging and glaucoma progression suggests  
377 potential for neuroprotective strategies targeting aging processes. Compounds like nicotinamide  
378 mononucleotide (NMN) and nicotinamide, precursors to NAD<sup>+</sup>, have shown promise in animal  
379 studies. Williams et al.<sup>38</sup> demonstrated that nicotinamide administration prevented glaucoma in  
380 aged mice and those with ocular hypertension. Recent pilot human studies have also shown  
381 potential benefits. Hui et al.<sup>39</sup> conducted a phase 2 clinical trial demonstrating that high-dose oral  
382 nicotinamide improved inner retinal function in glaucoma patients. Additionally, De Moraes et  
383 al.<sup>40</sup> reported that oral nicotinamide supplementation enhanced retinal ganglion cell function in  
384 patients with early-stage glaucoma. While these results are promising, larger and longer-term  
385 studies are needed to fully establish the efficacy and safety of these compounds in human  
386 glaucoma patients. Nonetheless, these findings, coupled with our observations on epigenetic age  
387 acceleration, highlight the potential of targeting aging processes as a novel therapeutic approach  
388 in glaucoma management.

389           While our study provides compelling evidence for the role of biological aging in  
390 glaucoma progression, several limitations must be acknowledged. Primarily, blood samples for  
391 epigenetic analysis were collected after progression had occurred, precluding the establishment  
392 of a causal relationship. Although we attempted to control for this by including follow-up time to  
393 blood collection in our multivariable models, prospective studies are needed to confirm the  
394 predictive value of epigenetic age acceleration in glaucoma progression. Another limitation is the  
395 potential impact of glaucoma treatment on our results. While we controlled for IOP in our  
396 models, the effects of various treatments on epigenetic age acceleration are unknown and could  
397 potentially confound our findings. Additionally, our study was conducted in a single center,  
398 which may limit the generalizability of our results to other populations.

399            In conclusion, this study provides the first evidence of an association between accelerated  
400 epigenetic aging and faster glaucoma progression. Our findings suggest that biological age, as  
401 measured by DNA methylation patterns, may be an important factor in determining an increased  
402 susceptibility to glaucomatous damage. Future prospective studies are needed to validate these  
403 findings and explore the potential of epigenetic age as a biomarker for glaucoma progression.  
404

## 405 REFERENCES

- 406 1. Weinreb RN, Aung T, Medeiros FA. The pathophysiology and treatment of glaucoma: a  
407 review. *JAMA* 2014;311(18):1901-11.
- 408 2. Susanna BN, Ogata NG, Jammal AA, et al. Corneal Biomechanics and Visual Field  
409 Progression in Eyes with Seemingly Well-Controlled Intraocular Pressure. *Ophthalmology*  
410 2019;126(12):1640-6.
- 411 3. Jammal AA, Berchuck SI, Thompson AC, et al. The Effect of Age on Increasing  
412 Susceptibility to Retinal Nerve Fiber Layer Loss in Glaucoma. *Invest Ophthalmol Vis Sci*  
413 2020;61(13):8.
- 414 4. Mitchell P, Smith W, Attebo K, Healey PR. Prevalence of open-angle glaucoma in  
415 Australia. The Blue Mountains Eye Study. *Ophthalmology* 1996;103(10):1661-9.
- 416 5. Varma R, Ying-Lai M, Francis BA, et al. Prevalence of open-angle glaucoma and ocular  
417 hypertension in Latinos: the Los Angeles Latino Eye Study. *Ophthalmology* 2004;111(8):1439-  
418 48.
- 419 6. Collaborative Normal-Tension Glaucoma Study Group. Comparison of glaucomatous  
420 progression between untreated patients with normal-tension glaucoma and patients with  
421 therapeutically reduced intraocular pressures. *Am J Ophthalmol* 1998;126(4):487-97.
- 422 7. Leske MC, Connell AM, Wu SY, et al. Distribution of intraocular pressure. The Barbados  
423 Eye Study. *Arch Ophthalmol* 1997;115(8):1051-7.
- 424 8. Rohtchina E, Mitchell P, Wang JJ. Relationship between age and intraocular pressure:  
425 the Blue Mountains Eye Study. *Clin Exp Ophthalmol* 2002;30(3):173-5.
- 426 9. Friberg TR, Lace JW. A comparison of the elastic properties of human choroid and sclera.  
427 *Exp Eye Res* 1988;47(3):429-36.
- 428 10. Quigley HA, Addicks EM. Regional differences in the structure of the lamina cribrosa  
429 and their relation to glaucomatous optic nerve damage. *Arch Ophthalmol* 1981;99(1):137-43.
- 430 11. Grossniklaus HE, Nickerson JM, Edelhauser HF, et al. Anatomic alterations in aging and  
431 age-related diseases of the eye. *Invest Ophthalmol Vis Sci* 2013;54(14):ORSF23-7.
- 432 12. Ramrattan RS, van der Schaft TL, Mooy CM, et al. Morphometric analysis of Bruch's  
433 membrane, the choriocapillaris, and the choroid in aging. *Invest Ophthalmol Vis Sci*  
434 1994;35(6):2857-64.
- 435 13. Flammer J, Orgul S, Costa VP, et al. The impact of ocular blood flow in glaucoma. *Prog*  
436 *Retin Eye Res* 2002;21(4):359-93.
- 437 14. Burgoyne CF, Downs JC, Bellezza AJ, et al. The optic nerve head as a biomechanical  
438 structure: a new paradigm for understanding the role of IOP-related stress and strain in the  
439 pathophysiology of glaucomatous optic nerve head damage. *Prog Retin Eye Res* 2005;24(1):39-  
440 73.
- 441 15. Gabelt BT, Kaufman PL. Changes in aqueous humor dynamics with age and glaucoma.  
442 *Prog Retin Eye Res* 2005;24(5):612-37.
- 443 16. Horvath S, Raj K. DNA methylation-based biomarkers and the epigenetic clock theory of  
444 ageing. *Nat Rev Genet* 2018;19(6):371-84.
- 445 17. Marioni RE, Shah S, McRae AF, et al. DNA methylation age of blood predicts all-cause  
446 mortality in later life. *Genome Biol* 2015;16(1):25.
- 447 18. Jammal AA, Berchuck SI, Mariottoni EB, et al. Blood Pressure and Glaucomatous  
448 Progression in a Large Clinical Population. *Ophthalmology* 2022;129(2):161-70.

- 449 19. Jammal AA, Thompson AC, Mariottoni EB, et al. Impact of Intraocular Pressure Control  
450 on Rates of Retinal Nerve Fiber Layer Loss in a Large Clinical Population. *Ophthalmology*  
451 2021;128(1):48-57.
- 452 20. Jammal AA, Thompson AC, Mariottoni EB, et al. Rates of Glaucomatous Structural and  
453 Functional Change From a Large Clinical Population: The Duke Glaucoma Registry Study. *Am J*  
454 *Ophthalmol* 2021;222:238-47.
- 455 21. Youssif AA, Onyekaba NA, Naithani R, et al. Social history and glaucoma progression:  
456 the effect of body mass index, tobacco and alcohol consumption on the rates of structural change  
457 in patients with glaucoma. *Br J Ophthalmol* 2024.
- 458 22. Leite MT, Rao HL, Zangwill LM, et al. Comparison of the diagnostic accuracies of the  
459 Spectralis, Cirrus, and RTVue optical coherence tomography devices in glaucoma.  
460 *Ophthalmology* 2011;118(7):1334-9.
- 461 23. Aryee MJ, Jaffe AE, Corrada-Bravo H, et al. Minfi: a flexible and comprehensive  
462 Bioconductor package for the analysis of Infinium DNA methylation microarrays.  
463 *Bioinformatics* 2014;30(10):1363-9.
- 464 24. Pidsley R, CC YW, Volta M, et al. A data-driven approach to preprocessing Illumina  
465 450K methylation array data. *BMC Genomics* 2013;14:293.
- 466 25. Horvath S. DNA methylation age of human tissues and cell types. *Genome Biol*  
467 2013;14(10):R115.
- 468 26. Hannum G, Guinney J, Zhao L, et al. Genome-wide methylation profiles reveal  
469 quantitative views of human aging rates. *Mol Cell* 2013;49(2):359-67.
- 470 27. Levine ME, Lu AT, Quach A, et al. An epigenetic biomarker of aging for lifespan and  
471 healthspan. *Aging (Albany NY)* 2018;10(4):573-91.
- 472 28. Lu AT, Quach A, Wilson JG, et al. DNA methylation GrimAge strongly predicts lifespan  
473 and healthspan. *Aging (Albany NY)* 2019;11(2):303-27.
- 474 29. Lin MT, Beal MF. Mitochondrial dysfunction and oxidative stress in neurodegenerative  
475 diseases. *Nature* 2006;443(7113):787-95.
- 476 30. Tezel G. Oxidative stress in glaucomatous neurodegeneration: mechanisms and  
477 consequences. *Prog Retin Eye Res* 2006;25(5):490-513.
- 478 31. Crowston JG, Kong YX, Trounce IA, et al. An acute intraocular pressure challenge to  
479 assess retinal ganglion cell injury and recovery in the mouse. *Exp Eye Res* 2015;141:3-8.
- 480 32. Kong YX, van Bergen N, Bui BV, et al. Impact of aging and diet restriction on retinal  
481 function during and after acute intraocular pressure injury. *Neurobiol Aging* 2012;33(6):1126  
482 e15-25.
- 483 33. Levkovitch-Verbin H, Vander S, Makarovsky D, Lavinsky F. Increase in retinal ganglion  
484 cells' susceptibility to elevated intraocular pressure and impairment of their endogenous  
485 neuroprotective mechanism by age. *Mol Vis* 2013;19:2011-22.
- 486 34. Liu B, McNally S, Kilpatrick JI, et al. Aging and ocular tissue stiffness in glaucoma. *Surv*  
487 *Ophthalmol* 2018;63(1):56-74.
- 488 35. Levine ME, Lu AT, Bennett DA, Horvath S. Epigenetic age of the pre-frontal cortex is  
489 associated with neuritic plaques, amyloid load, and Alzheimer's disease related cognitive  
490 functioning. *Aging (Albany NY)* 2015;7(12):1198-211.
- 491 36. McCartney DL, Stevenson AJ, Walker RM, et al. Investigating the relationship between  
492 DNA methylation age acceleration and risk factors for Alzheimer's disease. *Alzheimers Dement*  
493 (Amst) 2018;10:429-37.

- 494 37. Horvath S, Ritz BR. Increased epigenetic age and granulocyte counts in the blood of  
495 Parkinson's disease patients. *Aging (Albany NY)* 2015;7(12):1130-42.
- 496 38. Williams PA, Harder JM, Foxworth NE, et al. Vitamin B(3) modulates mitochondrial  
497 vulnerability and prevents glaucoma in aged mice. *Science* 2017;355(6326):756-60.
- 498 39. Hui F, Tang J, Williams PA, et al. Improvement in inner retinal function in glaucoma with  
499 nicotinamide (vitamin B3) supplementation: A crossover randomized clinical trial. *Clin Exp*  
500 *Ophthalmol* 2020;48(7):903-14.
- 501 40. De Moraes CG, John SWM, Williams PA, et al. Nicotinamide and Pyruvate for  
502 Neuroenhancement in Open-Angle Glaucoma: A Phase 2 Randomized Clinical Trial. *JAMA*  
503 *Ophthalmol* 2022;140(1):11-8.

504

505 **FIGURE LEGENDS**

506

507 **Figure 1.** Scatter plots illustrating the relationship between epigenetic age (y-axis) and  
508 chronological age (x-axis) for four epigenetic clocks: (A) Horvath, (B) Hannum, (C) PhenoAge,  
509 and (D) GrimAge. Each point represents an individual patient. Pearson correlation coefficients  
510 ( $r$ ) are shown for each clock. Epigenetic age was calculated using DNA methylation data from  
511 blood samples collected during the follow-up period. Chronological age is the age at blood  
512 collection.

513 **Figure 2.** Histograms depicting the distribution of epigenetic age acceleration values for (A)  
514 Horvath, (B) Hannum, (C) PhenoAge, and (D) GrimAge clocks in fast (black) and slow (grey)  
515 glaucoma progressors. Age acceleration was calculated as the residual from a linear regression of  
516 epigenetic age on chronological age. Positive values indicate an epigenetic age greater than  
517 chronological age.

518 **Figure 3.** Predicted probability of fast glaucoma progression based on Horvath age acceleration  
519 The curve shows the predicted probability of fast glaucoma progression (y-axis) as a function of  
520 Horvath age acceleration (x-axis), derived from the multivariable logistic regression model. Age  
521 acceleration was calculated as the residual from a linear regression of Horvath epigenetic age on  
522 chronological age. The shaded area represents the 95% confidence interval. The model is  
523 adjusted for sex, race, peak intraocular pressure, baseline mean deviation, central corneal

524 thickness and follow-up time until blood collection.

**Table 1.** Demographic and clinical characteristics of fast and slow glaucoma progressors.

Characteristic	Slow Progressors (n=100)	Fast Progressors (n=100)	P
Age at baseline (years)	61.8 ± 9.0	60.6 ± 11.8	0.43
Age at blood collection (years)	73.4 ± 8.3	71.7 ± 10.2	0.20
Sex (female), n (%)	59 (59%)	58 (58%)	0.89
Race (Black or African American), n (%)	21 (21%)	22 (22%)	0.86
Smoking status, yes, n (%)	5 (5%)	2 (2%)	0.25
Baseline MD (dB)	-3.52 ± 4.52	-6.05 ± 5.75	<0.001
Peak IOP (mmHg)	20.5 ± 5.4	23.8 ± 8.6	0.002
Mean IOP (mmHg)	15.3 ± 3.3	15.0 ± 3.1	0.39
CCT (µm)	548.7 ± 34.0	542.5 ± 45.9	0.28
Number of tests	8.1 ± 5.0	8.3 ± 4.4	0.81
Follow-up time (years)	11.0 ± 6.7	10.3 ± 6.1	0.45
Time to blood collection (years)	11.5 ± 6.6	11.4 ± 6.3	0.86
Average MD slope (dB/year)	0.01 ± 0.32	-0.63 ± 0.72	<0.001
Fastest MD slope (dB/year)	-0.10 ± 0.33	-1.06 ± 1.08	<0.001
Average RNFL slope (µm/year)	-0.30 ± 1.42	-0.99 ± 1.59	0.002
Fastest RNFL slope (µm/year)	-0.76 ± 1.37	-1.60 ± 1.86	<0.001

Values indicate mean ± standard deviation unless otherwise noted.

CCT: central corneal thickness, IOP: intraocular pressure, MD: mean deviation, RNFL: retinal nerve fiber layer thickness.

525



**Table 2.** Differences in epigenetic age acceleration between fast and slow glaucoma progressors.

<b>Age Acceleration (years)</b>	<b>Mean Difference</b>	<b>95% CI Lower</b>	<b>95% CI Upper</b>	<b>P-value</b>
<b>Horvath</b>	2.93	1.48	4.39	<0.001
<b>Hannum</b>	1.24	0.03	2.46	0.045
<b>PhenoAge</b>	1.06	-0.51	2.64	0.185
<b>GrimAge</b>	1.49	-0.17	3.14	0.079

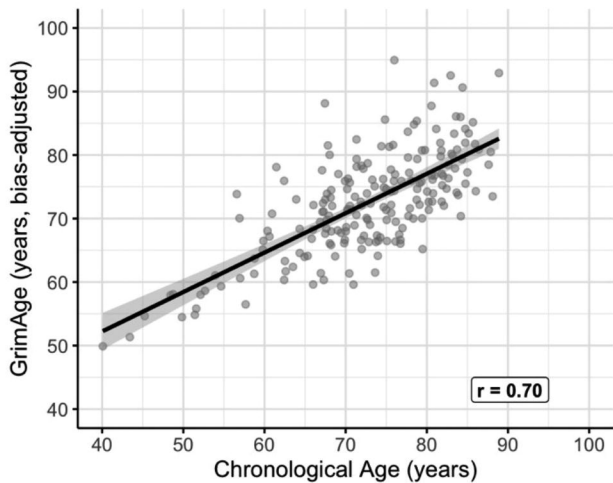
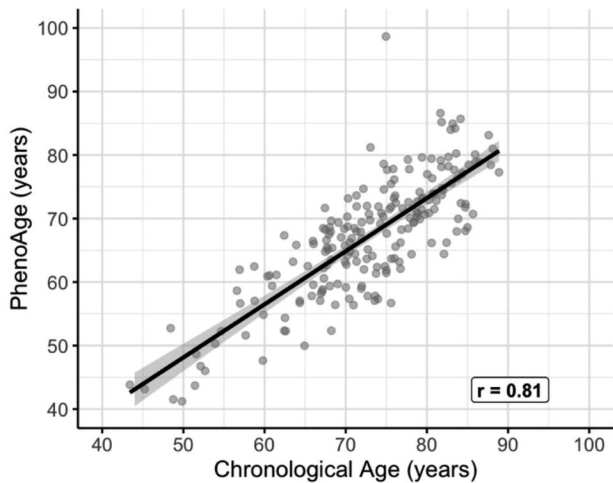
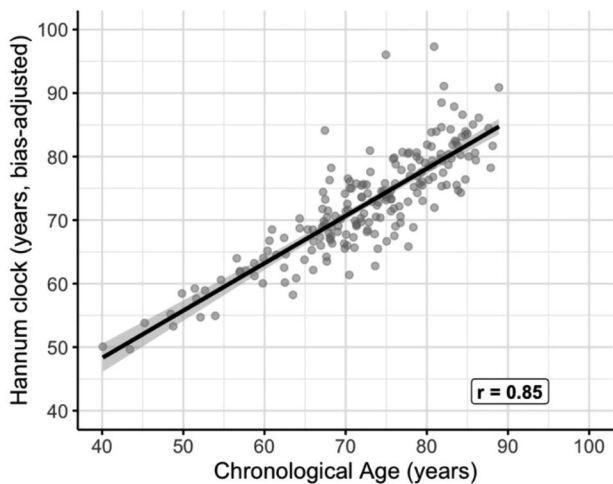
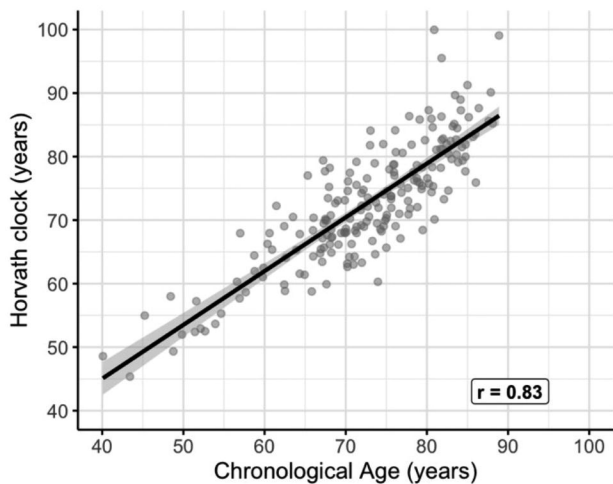
Note: Age acceleration measures correspond to residuals of the regression between epigenetic age and chronologic age at time of blood collection. Mean difference is calculated as (mean of fast progressors) - (mean of slow progressors). Positive values indicate that fast progressors had higher age acceleration than slow progressors. CI: confidence interval.

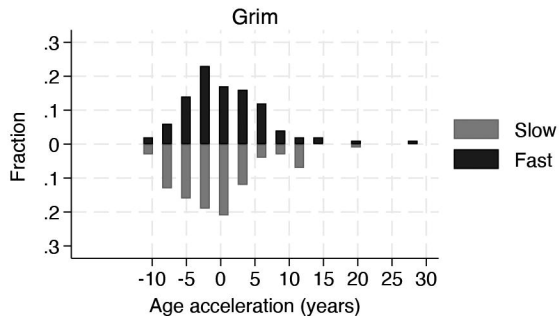
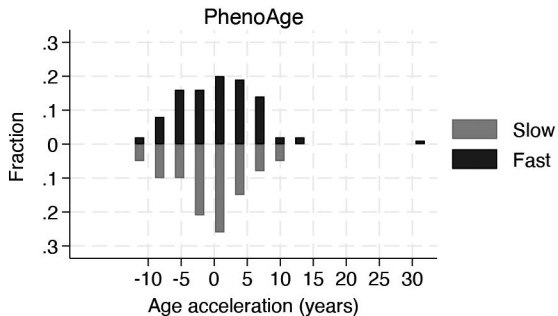
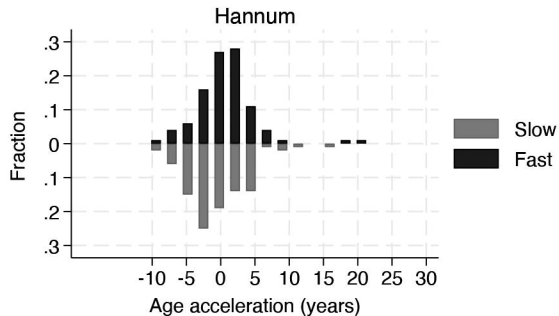
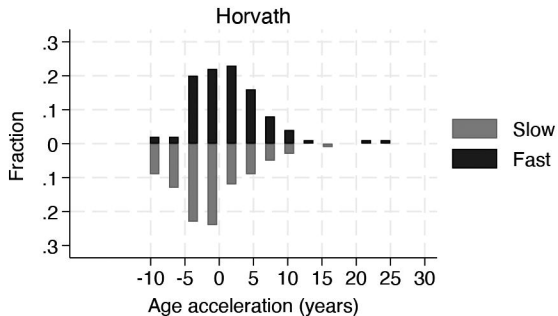
**Table 3.** Results of multivariable logistic regression models for the association between epigenetic age acceleration and fast glaucoma progression.

Variable	Horvath		Hannum		PhenoAge		Grim	
	OR (95% CI)	P	OR (95% CI)	P	OR (95% CI)	P	OR (95% CI)	P
Age Acceleration, y	1.15 (1.07-1.23)	<0.001	1.07 (1.00-1.15)	0.049	1.04 (0.99-1.10)	0.141	1.07 (1.01-1.14)	0.034
Sex, male	1.56 (0.79-3.07)	0.197	1.47 (0.76-2.87)	0.254	1.29 (0.68-2.45)	0.436	1.59 (0.81-3.15)	0.181
Race, Black/AA	1.03 (0.48-2.23)	0.935	1.11 (0.52-2.34)	0.789	0.92 (0.42-1.98)	0.824	0.82 (0.37-1.79)	0.617
Peak IOP	1.10 (1.04-1.15)	<0.001	1.09 (1.04-1.15)	0.001	1.09 (1.04-1.15)	0.001	1.09 (1.04-1.14)	0.001
Baseline MD, per dB lower	1.13 (1.05-1.22)	0.001	1.13 (1.05-1.21)	0.001	1.13 (1.05-1.21)	0.001	1.12 (1.05-1.20)	0.001
CCT, per 40µm thinner	1.23 (0.88-1.70)	0.223	1.19 (0.87-1.64)	0.274	1.19 (0.87-1.63)	0.282	1.26 (0.91-1.74)	0.164
Follow-up time, y	1.03 (0.98-1.08)	0.312	1.02 (0.97-1.07)	0.471	1.02 (0.97-1.07)	0.504	1.02 (0.97-1.07)	0.380
Smoking, yes	0.46 (0.08-2.63)	0.380	0.56 (0.10-3.17)	0.512	0.58 (0.10-3.28)	0.537	0.35 (0.06-2.14)	0.255

AA: African-American, CCT: central corneal thickness, CI: confidence interval, IOP: intraocular pressure, MD: mean deviation, OR: odds ratio. Follow-up time: follow-up time until blood collection







# Predicted Probability of Fast Glaucoma Progression

Based on Horvath Age Acceleration

